Fabrication of Stable Nanocylinder Arrays in Highly Birefringent Films of an Amphiphilic Liquid-Crystalline Diblock Copolymer

Haifeng Yu*,[†] and Takaomi Kobayashi[‡]

Top Runner Incubation Center for Academia-Industry Fusion and Department of Materials Science and Technology, Nagaoka University of Technology, 1603-1 Kamitomioka, 940-2188 Nagaoka, Niigata, Japan

ABSTRACT An amphiphilic liquid-crystalline diblock copolymer (LCDC) with a highly birefringent cyanobiphenyl (CB) group as a mesogen was prepared by atom-transfer radical polymerization. The obtained LCDC showed a well-defined structure and a narrow molecular-weight distribution. In its spin-coated films, both liquid-crystalline (LC) alignment and microphase-separated nanostructures were systematically studied. Random LC arrangement and ambiguous microphase separation were observed in as-prepared films because of the high viscosity at room temperature. Upon annealing of the films in an isotropic phase of the LCDC, the CB mesogens self-organized into a smectic texture of a conic fan and the microphase separation proceeded completely. It is the supramolecular cooperative motion that enables the LCDC to hierarchically assemble into a regular patterning of normally aligned nanocylinders to the substrate, dispersed in the out-of-plane-oriented mesogens. With the help of homogeneous alignment of the CB groups induced by a rubbing technique, uniform patterning of highly ordered nanocylinders parallel to the rubbing direction was successfully fabricated in the plane. The fabricated perpendicular and parallel patterning of nanocylinders dispersed in the highly birefringent films with the CB block as the majority phase show good stability under room light, indicating their potential applications as nanotemplates for preparing advanced nanoscaled materials.

KEYWORDS: amphiphilic diblock copolymer • liquid crystal • microphase separation • supramolecular cooperative motion • self-organization • nanotechnology

INTRODUCTION

Functional block copolymers with liquid-crystalline (LC) properties are one type of novel macromolecule with industrial and academic interests because they offer the opportunities study on the organic nanostructure formation and control under the influence of more than one driving force. Generally, microphase-separated nanostructures should effect functionality (e.g., LC ordering), and vice versa, and specific functionalities (e.g., LC properties) should exert influence on the diverse nanostructures in the LC block copolymers (1−12). In thin films of LC diblock copolymers (LCDCs), the LC block can form spheres, cylinders, lamellae domains, and a continuous phase with an increase in its volume ratio upon microphase separation. LCDCs show behaviors similar to those of amorphous block copolymers when the LC segment forms the minority phase upon microphase separation, and the LC performance could not be detected by thermal analysis and polarizing optical microscope (POM) when the mesogen self-organizes into the minority phase of nanoscopic spheres (13, 14). On the contrary, LCDCs with the mesogenic block in the majority phase exhibit almost the same LC properties as their corresponding LC homopolymers. In this case, the interplay function between the microphase separation and the elastic deformation of LC ordering, generally known as supramolecular cooperative motion (SMCM) (15, 16), plays an important role in the formation of hierarchical structures in LCDC films, which enables their microphase separation to be controlled by manipulation of the alignment of the LC block. Our previous work demonstrated that the phase-segregated nanodomains in the LCDC films might be controlled in an ordered array along with the alignment direction of the LC matrix (15, 16).

Using an azobenzene as both a mesogen and a photoresponsive group, we prepared a series of novel amphiphilic LCDCs consisting of flexible poly(ethylene oxide) (PEO) as a hydrophilic segment and polymethacrylate containing an azobenzene moiety in the side chain as hydrophobic LC segments (7, 15, 16). Upon microphase separation, the PEO-based LCDCs showed regular patterning of a PEO nanocylinder array, periodically dispersed in the azobenzene LC matrix. Although the PEO nanocylinder array was successively controlled in macroscopic ordering by either the rubbing technique (15) or a polarized laser beam (16), it showed a poor optical durability. To improve the stability of the microphase-separated nanostructures, a nonphotosensitive aramid moiety was introduced as a mesogen to form successive hydrogen bonds in the LC matrix (17). It is a pity that the obtained aramid-containing LCDC showed low birefringence and poor solubility because of the strong function of inter- and intramolecular hydrogen bonds (17),

---

* To whom correspondence should be addressed. E-mail: yuhaifeng@mst.nagaokaut.ac.jp. Tel: +81-0258-47-8416. Fax: +81-0258-47-9300.

Received for review July 30, 2009 and accepted November 6, 2009

[†] Top Runner Incubation Center for Academia-Industry Fusion.

[‡] Department of Materials Science and Technology.

DOI: 10.1021/am900509v

Scheme 1. Synthetic Route and Properties of the CB-Containing Diblock Copolymer PEO-*b*-PM11CB Used in This Study[a]

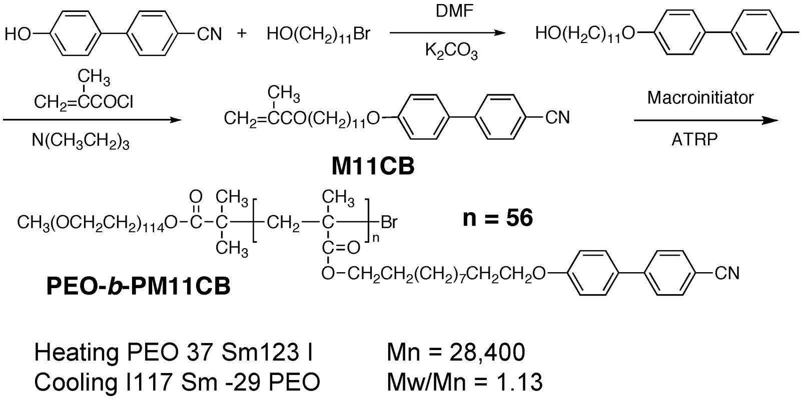

[a] Sm represents a smectic LC phase. M_n and M_w are the number- and weight-average molecular weights, respectively.

which limits their further applications in nanopatterning, template syntheses and grating devices. In this paper, a cyanobiphenyl (CB) group, well-known for its high birefringence (18), was used as a photoinactive mesogen to replace the aramid moiety in LCDCs. Because there is no formation of hydrogen bonds among CBs, the solubility in the organic solvent might be improved for the CB-containing LCDC. Furthermore, its nonphotoresponse to visible light could make the phase-segregated nanostructures in the designed LCDC exhibit high stability under room light. It is expected that stable PEO nanocylinders with a long periodicity can be obtained in highly birefringent films of the CB-containing LCDC.

EXPERIMENTAL SECTION

The synthesis of the monomer M11CB and the corresponding diblock copolymer PEO-*b*-PM11CB is illustrated in Scheme 1.

11-(4-Cyanobiphenyloxy)undecyl Methacrylate (M11CB). Monomer M11CB was prepared by the reaction between 4-cyano-4′-hydroxybiphenyl and 11-bromoundecan-1-ol and the following Schotten−Baumann reaction with methacryloyl chloride. ^{1}H NMR (δ, $CDCl_3$, ppm): 1.25−1.45 (m, 14H), 1.58 (t, 2H), 1.84 (t, 2H), 1.94 (s, 3H), 4.0 (t, 2H), 4.15 (t, 2H), 5.58 (d, 1H), 6.08 (d, 1H), 6.95 (d, 2H), 7.55 (d, 2H), 7.76 (q, 4H). UV−vis (chloroform): $\lambda_{max} = 297$ nm. DSC: K 70.4 Sm 78.9 I.

PEO Macroinitiator (PEO-Br). The macroinitiator PEO-Br was prepared by the Schotten−Baumann reaction between 2-bromo-2-methylpropionyl chloride and a PEO monomethyl ether (M_n = 5000) in the presence of triethylamine in a solution of CH_2Cl_2 with a yield of 32%. The number-average molecular weight (M_n) and the polydispersity index (M_w/M_n) measured with gel permeation chromatography (GPC) were 7400 and 1.02, respectively. ^{1}H NMR (δ, $CDCl_3$, ppm): 4.33 (d, 2H), 3.86 (t, 2H), 3.73 (m, 158H), 3.62 (t, 2H), 3.41(t, 2H), 3.38 (s, 3H), 1.94 (s, 6H). DSC: K 58.6 I.

Diblock Copolymer (PEO-*b*-PM11CB). PEO-*b*-PM11CB was prepared by atom-transfer radical polymerization (ATRP) (9, 17). Cu^ICl (29.7 mg, 0.30 mmol), PEO-Br (0.5 g, 0.1 mmol), and M11CB (3.13 g, 7.5 mmol) were mixed in a 25 mL ampule, degassed and filled with argon. The ligand 1,1,4,7,10,10-hexamethyltriethylenetetramine (69.0 mg, 0.3 mmol) in anisole (30.0 mL) was added. The mixture was degassed by three freeze−pump−thaw cycles and sealed in a vacuum, placed in an oil bath preheated at 80 °C for 24 h. Then the solution was passed through a neutral Al_2O_3 column to remove the catalyst. The filtrate was precipitated into hot methanol. The block copolymer was collected and dried in a vacuum. Yield: 2.6 g (72%). M_n(GPC) = 28 400. M_w/M_n = 1.13. ^{1}H NMR (δ, $CDCl_3$, ppm): 7.61 (d, 2H), 7.57 (d, 2H), 7.46 (d, 2H), 6.92 (d, 2H), 3.93 (m, 4H), 3.66 (m, 456H), 1.82−1.27 (m, 18H), 1.09−0.84 (m, 3H). UV−vis (chloroform): $\lambda_{max} = 298$ nm.

Film Preparation and Treatment. To study the microphase-separated behavior and the LC alignment, three kinds of PEO-*b*-PM11CB films with a thickness of about 200 nm were prepared, respectively, including as-prepared, annealed, and rubbing-treated films.

The as-prepared films were prepared by spin-coating a 2 g/L tetrahydrofuran (THF) solution on clean glass substrates without any pretreatment. The rotational speed was controlled at 500 rpm for 10 s and then 2000 rpm for another 30 s. After the solvent was removed at room temperature, the copolymer films were dried in a vacuum oven for 24 h at room temperature.

The annealed films were prepared by putting the dried copolymer films in a vacuum oven with a well-controlled hot stage and annealed at 140 °C for 24 h. To obtain good microphase-separated nanostructures, both the heating and cooling rates were carefully controlled at 1 °C/min.

To fabricate rubbing-treated films, clean glass substrates coated with polyimide films were first prepared by spin coating with 3 wt % poly(amic acid) solutions in *N*,*N*-dimethylformamide (DMF) at 500 rpm for 5 s and 3000 rpm for 30 s, and then they were soft-baked at 100 °C for 1 h and hard-baked at 250 °C for 2 h to remove the solvent and cure for imidization. The chemical structure of the polyimide used in this experiment is as follows.

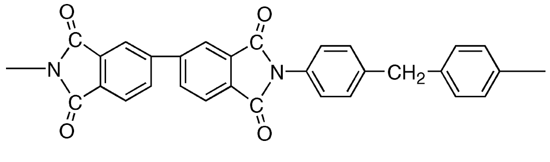

Using a rubbing machine, the polyimide film layers were mechanically rubbed with a rubbing cloth in a unidirectional way. Subsequently, the diblock copolymer in a THF solution was spin-coated on the glass surfaces coated with the above-mentioned rubbed polyimide films to prepare oriented copolymer films. After the solvent was removed at room temperature, the copolymer film was also annealed at 140 °C in a vacuum oven for 24 h. Similarly, both heating and cooling rates were controlled at 1 °C/min. Then polarized UV−vis absorption spectra and POM observation were used to characterize the anisotropy of the rubbing-treated films.

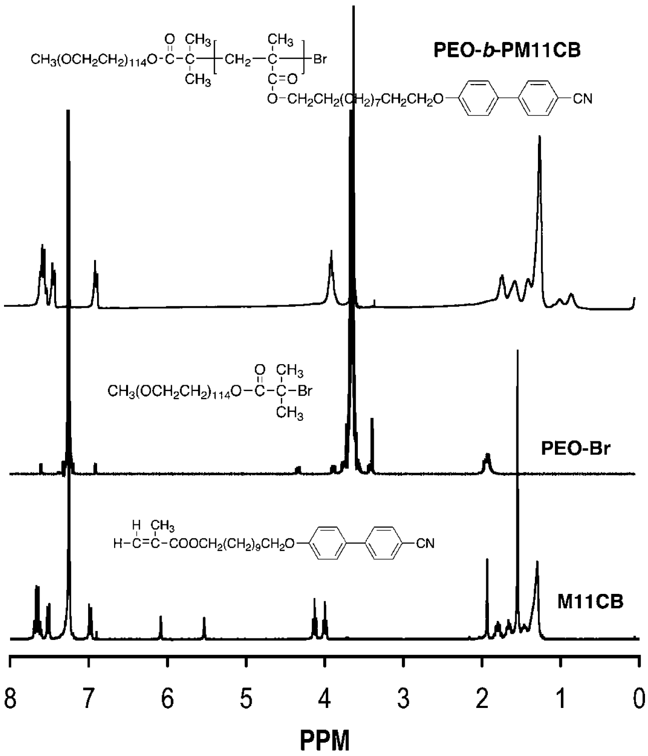

FIGURE 1. ^{1}H NMR spectra of the monomer M11CB, the macroinitiator PEO-Br, and the diblock copolymer PEO-*b*-PM11CB.

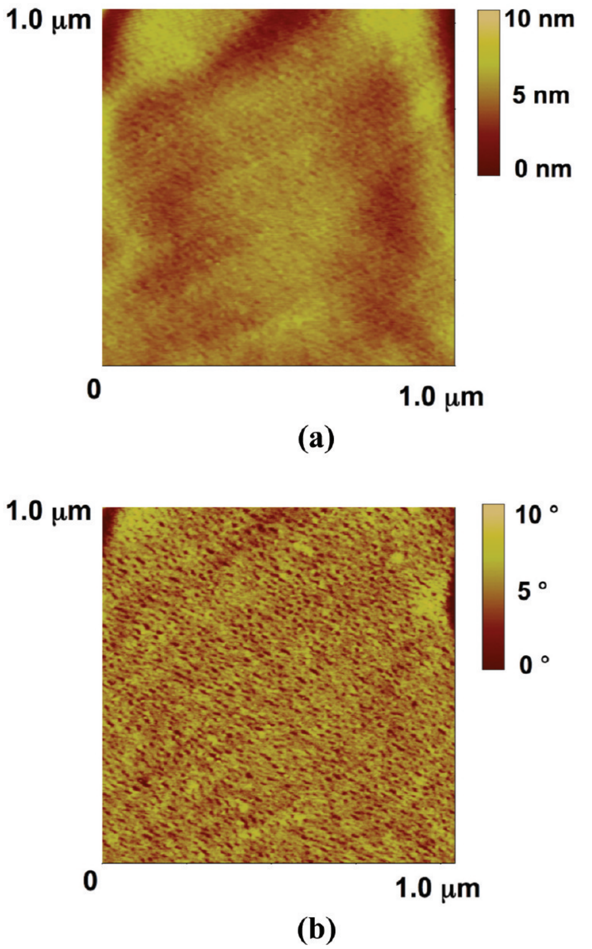

FIGURE 2. AFM height (a) and phase (b) images of the as-prepared films without annealing.

RESULTS AND DISCUSSION

Synthesis and Characterization of Materials. To obtain regularly ordered nanostructures in microphase-separated films of block copolymers, each segment in the block copolymers should have a well-defined structure (a narrow molecular-weight polydispersity) and has to be larger than a certain minimum molecular weight. Scheme 1 gives the synthetic route of the CB-containing diblock copolymer PEO-*b*-PM11CB, in which a bromo-substituted PEO (PEO-Br) with about 114 repeating units was used as the macroinitiator to undergo an ATRP reaction of the monomer M11CB (17, 19). Both GPC curves and NMR spectra were used to characterize the structure and molecular weight of the obtained LCDC. Figure 1 shows the NMR spectra of the monomer M11CB, the macroinitiator PEO-Br, and the diblock copolymer PEO-*b*-PM11CB in deuterated chloroform. Obviously, the well-specified molecular structure of PEO-*b*-PM11CB can be easily assigned in the NMR spectra, and about 56 repeating units of the CB block were estimated by integration of the phenyl proton NMR peak at 6.92 ppm of the CB group to that of the oxyethylene protons of PEO at 3.66 ppm. The GPC curve with standard polystyrenes in chloroform as the eluent gives a molecular weight of 28 400 (M_n) and a narrow polydispersity index of 1.13, which coincide with the estimated results from NMR analysis, indicating a well-defined molecular structure of the obtained LCDC.

As expected from the molecular design, the obtained PEO-*b*-PM11CB showed good solubility in organic solvents, such as THF, chloroform, toluene, DMF, and anisole, which is different from the aramid-containing LCDC only dissolving in polar solvents owing to the existence of successive hydrogen bonds (17). In its UV—vis absorption spectrum, only one peak appeared at the band of about 298 nm, due to the absorption of CB groups. No absorption peak was detected in the range of 400—700 nm, indicating its photo-inert feature to visible light. Two phase-transition peaks upon heating appeared at 37 and 123 °C in its thermogram by differential scanning calorimetry (DSC), respectively, corresponding to the PEO melting point to smectic LC to isotropic phase. Upon cooling, the clearing point appeared at 117 °C because of the overcooling effect (11). Interestingly, the PEO melting point was observed at −29 °C, which might be attributed to the confined crystallization by microphase separation (16).

As-Prepared Films. Because of the difference in the elastic modulus between the hydrophilic PEO block and the hydrophobic mesogenic segment, the microphase-separated structures in the as-prepared PEO-*b*-PM11CB films can be measured by atomic force microscopy (AFM) in tapping mode at room temperature (15—17). As shown in Figure 2a, an undulation of the surface height was less than 10 nm in the AFM height image, indicating a smooth surface of the spin-coated films. Although microphase separation can be dimly observed from the AFM phase image (Figure 2b), the obtained nanostructures were unclear and irregular. Generally, block copolymers with covalently jointed immiscible polymeric blocks form microphase-segregated structures

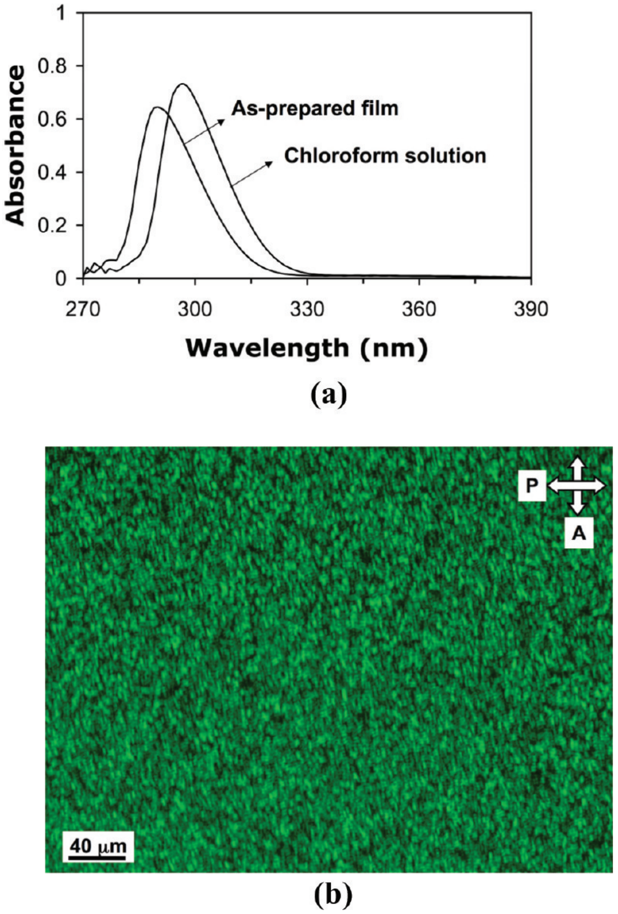

(a)

(b)

FIGURE 3. UV−vis absorption spectra (a) and POM image (b) of the as-prepared films: P, polarizer; A, analyzer.

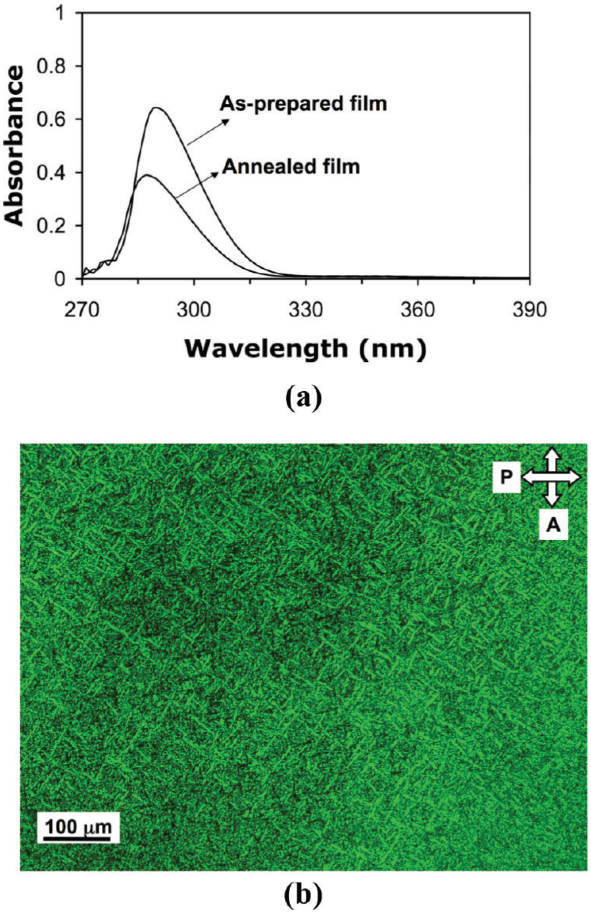

(a)

(b)

FIGURE 4. UV−vis absorption spectra (a) and POM image (b) of the annealed films.

because an unfavorable mixing enthalpy and a very small mixing entropy drive the block copolymer system into phase separation while the covalent bond between these two blocks prohibits the system from undergoing microphase segregation (20, 21). In the as-prepared LCDC films, the microphase separation occurred, accompanied by solvent evaporation in the process of spin coating. However, thermodynamically controlled microphase segregation cannot be completed thoroughly at room temperature because of the high viscosity of the LCDC in the film state, resulting in the ambiguous nanostructure shown in Figure 2b.

Figure 3a shows UV−vis absorption spectra of the block copolymer in the as-prepared film and the chloroform solution. Only the CB groups showed one absorption peak at the band of 298 nm in the chloroform solution, and its maximum absorption shifted to 292 nm in the solid film state. Moreover, no alignment of the CB groups was observed with POM, indicating their random arrangement in the as-prepared films. Although a birefringent texture can be observed in Figure 3b, it exhibited a glassy LC phase.

Annealed Films. To lower the viscosity of the PEO-*b*-PM11CB films and enable the microphase separation to proceed completely, the spin-coated films were annealed at 140 °C for 24 h, a little higher than the LC-to-isotropic phase transition temperature. As shown in Figure 4a, the UV−vis maximum absorption peak of the as-prepared films at 292 nm decreased greatly after annealing, probably attributed to the out-of-plane alignment of the CB mesogens, which is similar to our previously reported results (15−17). Moreover, a blue shift of about 6 nm appeared after annealing, which might be due to the formation of H-aggregation of CB moieties (22). Generally, the process of slowly cooling the annealed films to induce an isotropic-to-LC phase transition plays an importation role in the self-organization of the CB mesogens. A focal conic fan texture was clearly observed in the POM image shown in Figure 4b, indicating a smectic LC phase (9). Furthermore, there is no information about the PEO blocks (crystals) from the POM observation because the PEO block formed a nanoscaled phase domain, embedded in the continuous phase of the mesogenic CB block upon microphase separation, which is far beyond the resolution of the present POM.

On the one hand, the annealing of LCDC films greatly decreased the viscosity, enabling the microphase separation to thermodynamically proceed at the fluidlike isotropic phase. On the other hand, careful control of the slow cooling after annealing made the mesogen self-organize into good texture. Such inherent smectic LC ordering with layered structures might plays a key role in the thermally induced out-of-plane alignment of the CB mesogens, which exerted influences on the microphase-separated nanostructures. As shown in Figure 5, explicitly dotted nanostructures were clearly observed in the AFM images of the annealed LCDC films. Considering the composition of the obtained block

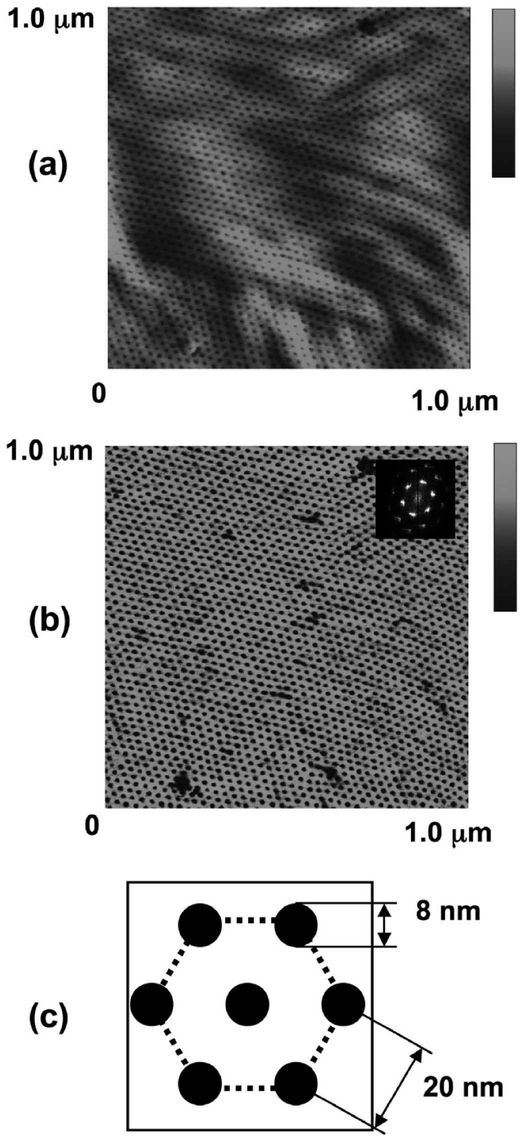

FIGURE 5. AFM height (a) and phase (b) images of annealed LCDC films and schematic illustration of the microphase separation (c). The inset of the AFM phase image b is the FFT.

copolymer, although the repeating units of PEO (114) are much more than those of the CB block (56), the PEO block still constitutes the minority component in the microphase separation. In the present PEO-*b*-PM11CB, the PEO block is well-known for its crystallization and strong inter- or intramolecular interaction (hydrogen bonds), while the other block of CB mesogens has inherent LC properties of self-organization, long-range ordering, and anisotropy in various physical properties (23). Therefore, strong molecular interactions exist in both of the polymeric constituent segments of the LCDC, which makes its microphase separation different from that of other block copolymers with relatively weak molecular interactions (7−17). By supramolecular self-assembly, the PEO blocks segregated into hydrophilic nanocylinders of about 8 nm diameter and 20 nm periodicity dispersed in a matrix of CB mesogens. The fast Fourier transform (FFT) image shown in Figure 5b indicates a hexagonal packing of the PEO nanocylinders. Combined with the out-of-plane alignment of the CB mesogens, the perpendicular orientation and highly ordered arrangement of microphase-separated PEO cylinders might be perpendicular to the smectic LC layers. Figure 5c gives a schematic illustration of the microphase-separated PEO nanocylinders in the annealed films.

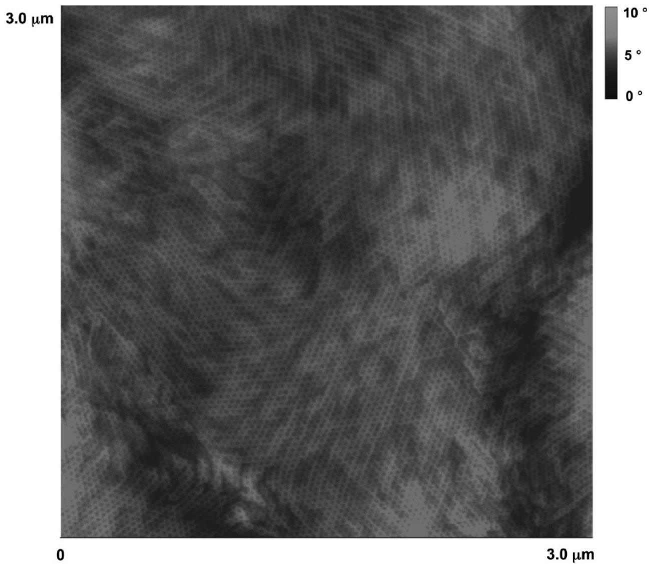

FIGURE 6. AFM phase image of the annealed LCDC films in a large area.

Figure 6 gives microphase-separated nanostructures only in 3 μm × 3 μm because of the limited resolution of the AFM used. Actually, such a dotted patterning of PEO nanocylinders can be achieved in an arbitrary area, depending on the size of the substrates. For microphase separation in films of amorphous block copolymers, electric or magnetic fields (24, 25), the temperature gradient (26), crystallization (27), the modified surface of the substrates (28), shearing (29), solvent evaporation (30), and roll casting (31) have been explored to obtain long-range orders. Although no especially external driving forces were exerted on the LCDC films, the regularly periodic arrangements of the nanocylinders can be obtained in a macroscopic scale. That is to say, it is the LC characteristics that enable the LCDC to self-organize into the ordered arrangement of microphase-separated nanostructures, whereas such a self-assembled process does not exist in films of amorphous block copolymers. Because the perpendicular orientation of the ordered PEO nanocylinder array might be formed with the help of the out-of-plane alignment of the CB mesogens, the microphase separation in the LCDC can be manipulated by control of the LC alignment under the function of SMCM. Such reliably ordered nanostructures in a large region are crucial for their further applications as nanotemplates (30).

Rubbing-Treated Films. It is well-known that the LC alignment technique by rubbed polyimide films is one of the most effective ways to homogeneously align LC molecules, which has been widely used in the production of LC displays (32). To prepare a parallel patterning of PEO nanocylinders in block copolymer films, a commercially available rubbing method was used. After thermal treatment, the rubbed polyimide films induced homogeneous alignment of the CB mesogens in the LCDC films, and an intensive anisotropy

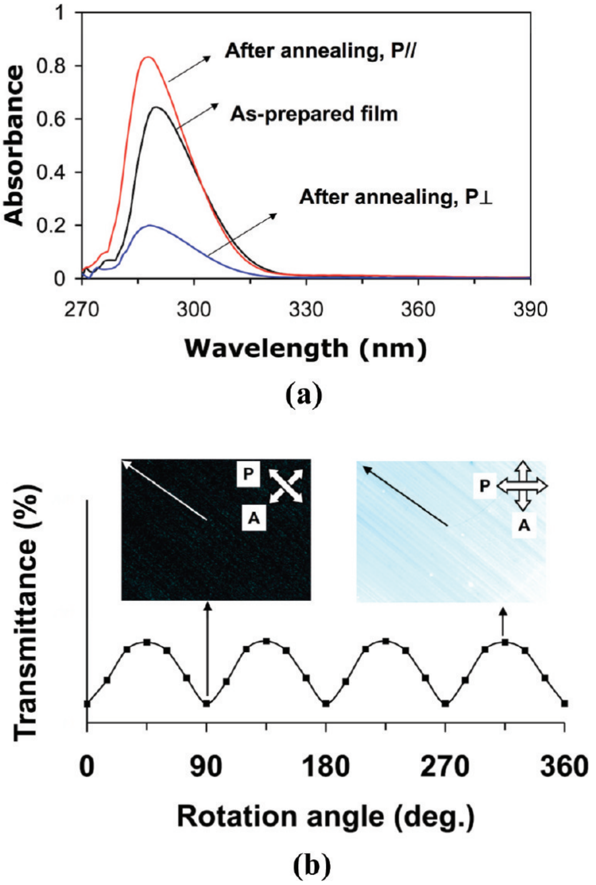

(a)

(b)

FIGURE 7. UV−vis absorption (a) and anisotropy (b) of the rubbing-treated films. $P_\perp$ and $P_\parallel$ in part a are the absorption curves perpendicular and parallel to the rubbing direction, respectively. The arrows in part b indicate the rubbing direction. The area of POM pictures in part b is 400 μm × 300 μm.

in its polarized UV−vis absorption spectra was observed in Figure 7a. Similarly, the formation of H-aggregation of CB mesogens induced a blue shift in the UV−vis absorption peak. The order parameter (S) of the aligned film can be calculated by $S = (A_\parallel - A_\perp)/(A_\parallel + 2A_\perp)$, where $A_\perp$ and $A_\parallel$ are absorbances perpendicular and parallel to the rubbing direction, respectively. Then $S = 0.51$ was obtained at 286 nm, which is similar to the AZ-containing diblock copolymers (16). When the rubbing-treated film was placed between a set of two-crossed polarizer and analyzer, the LC alignment was checked by measuring the transmittance (T), as a function of the rotation angle between the rubbing direction and the polarizer. If the LC alignment is homogeneous, T should satisfy the following equation:

$$T = \frac{I}{I_0} = \sin^2(2\theta)\,\sin^2\left[\frac{\pi d \Delta n}{\lambda}\right] \qquad (1)$$

where θ is the angle between the direction of the LC alignment and the polarization of the polarizer, d is the film thickness, Δn is the birefringence of the films, and λ is the wavelength of the probe light (633 nm). As shown in Figure 7b, T exhibited a sinusoidal-like curve, changing periodically with 90° for the rotation angle. Accordingly, the CB mesogens were in-plane-aligned along the rubbing direction because T showed a maximum value ($T_{\max} = 1.0\%$) when the sample film was tilted by 45° or 135° and so on, with respect to the rubbing direction and polarizer, whereas T showed a minimum value at 0° or 90° and so on. The LCDC film showed a high birefringence of about 0.20, evaluated by eq 1. Generally, such a high birefringence cannot be obtained with amorphous block copolymers (15, 16).

As expected from the microphase separation under the function of SMCM, the PEO nanocylinder array also showed an intensive anisotropy in the highly birefringent films. The alignment of the PEO nanocylinder array, coinciding with the LC orientation, was clearly observed in the AFM height and phase images shown in Figure 8. The inset FFT image of Figure 8b demonstrated a parallel patterning of the PEO nanocylinders along the rubbing direction in the plane of the substrate. Such periodic nanostructures might be achieved by the interplay process between the LC ordering of the homogeneously aligned CB mesogens and the self-assembly of the amphiphilic diblock copolymers (7−17), which leads to an ordered parallel array along the rubbing direction. The obtained PEO nanocylinder array is very interesting because parallel processes for the patterning of densely packed nanostructures are often required for many diverse areas of nanotechnology (33).

Similar to the hexagonal patterning of normally oriented nanocylinders, the parallel array of PEO nanocylinders also can be fabricated over several centimeters in our experimental conditions, which have been confirmed by acquiring AFM images spaced by 100 μm over the whole substrate. Owing to the AFM resolution, an image of perfectly aligned nanocylinders in an area of 3 μm × 3 μm is provided in Figure 8c.

In the prepared LCDC films, the LC alignment and microphase-separated nanostructures can be schematically illustrated in Figure 9. In the as-prepared films, the CB mesogens are randomly distributed and the microphase separation occurred partly because of the high viscosity of the films. Upon annealing, the smectic CB mesogens showed out-of-plane arrangement, leading to a hexagonal packing of PEO nanocylinders normal to the substrate, obeying the function of SMCM. On the surface of the substrate coated with rubbed polyimide films, both the highly birefringent CB moieties and PEO nanocylinders in the anisotropic films were aligned along the rubbing direction. The perpendicular and parallel patterning of obtained PEO nanocylinder arrays showed good stability under room light, and no obvious change in the nanostructures was detected after being stored for several months. Actually, the pattering of the PEO nanocylinder array was stabilized by the majority phase in the LC state. At an elevated temperature below the clearing point of the CB block, the PEO nanocylinders can remain in their array even if PEO is in its isotropic phase, separately dispersed in the mesogenic matrix.

CONCLUSION

A well-defined LCDC with highly birefringent CBs as mesogens was prepared, and then its microphase separation and LC alignment were systematically studied in as-prepared, annealed, and rubbing-treated films, respectively. With the help of highly birefringent CB mesogens, the

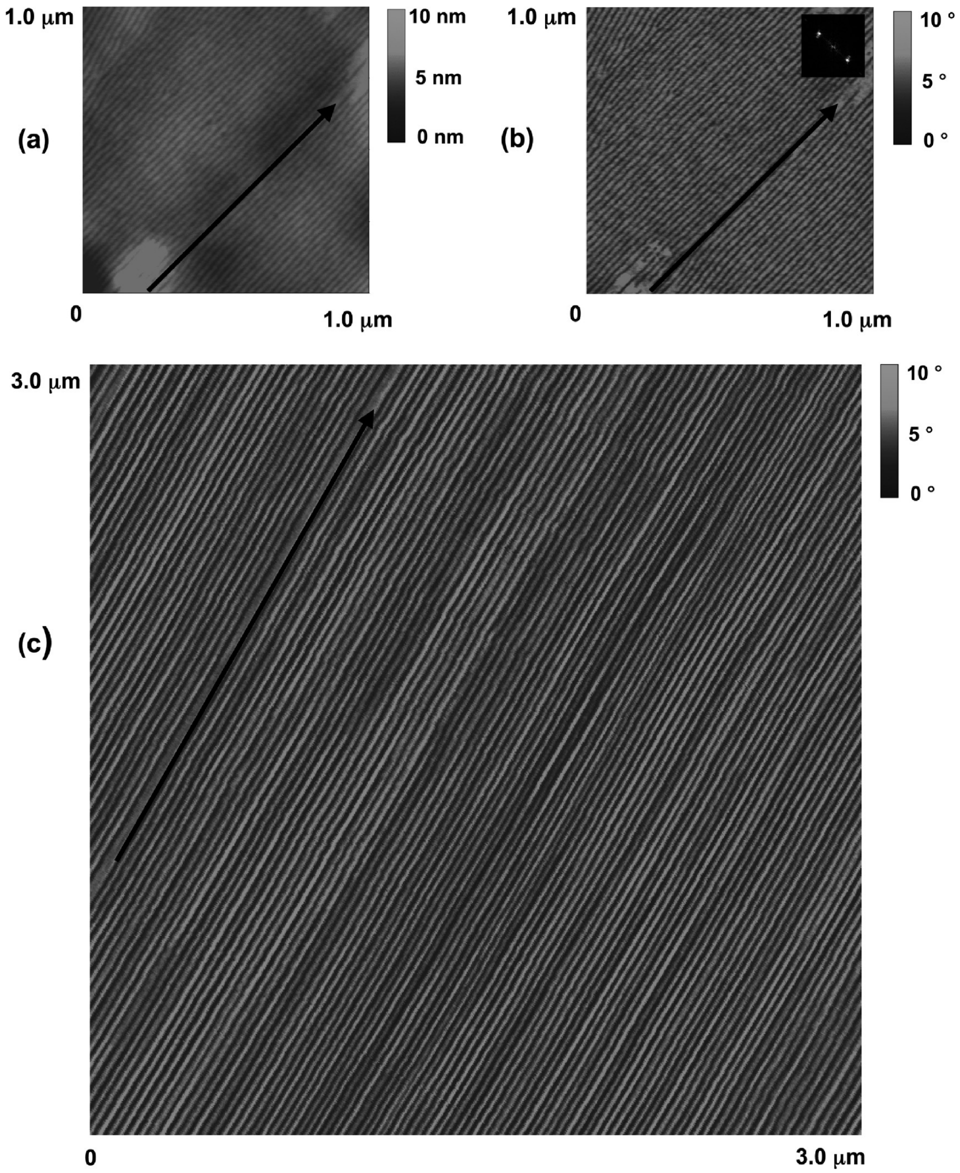

FIGURE 8. AFM height (a) and phase (b and c) images of annealed LCDC films. The inset of the AFM phase image is the FFT. The arrows indicate the rubbing direction.

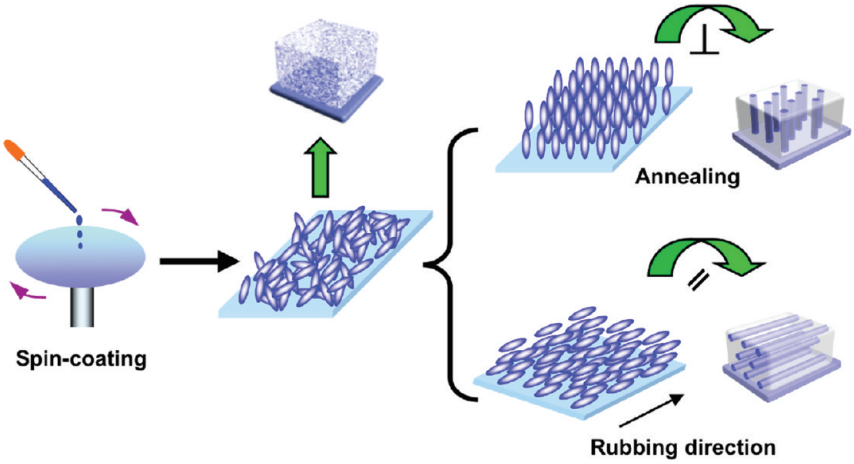

FIGURE 9. Schematic illustration of the LC alignment and the microphase separation in the highly birefringent LCDC films.

perpendicular and parallel patterning of ordered PEO nanocylinder arrays were successfully obtained under the function of SMCM. Such well-ordered arrays of nanocylinder domains composed of crystallizable PEO, dispersed in intensively anisotropic films with the highly birefringent CB block as the majority phase, can be regarded as a kind of "hybrid crystal", finely combining periodic ordering of a polymer LC with regular packing of the PEO nanocylinders. By the SMCM, the "hybrid crystal" shows ordered hydrophilic nanostructures in a macroscopic scale and a high birefringence from the hydrophobic mesogens, which might provide nanopatterned materials with a specially designed optical performance. The results indicate that the obtained LCDCs with highly birefringent CB mesogens can be used as reliable nanotemplates for preparing advanced materials with multifunctions.

Acknowledgment. We are grateful to the special coordination fund from MEXT of Japan, which supports the activities of "Promotion of Independent Research Environment for Young researchers".

REFERENCES AND NOTES

(1) Lee, M.; Cho, B. K.; Zin, W. C. *Chem. Rev.* **2001**, *101*, 3869.
(2) Walther, M.; Finkelmann, G. *Prog. Polym. Sci.* **1996**, *21*, 951.
(3) Mao, G.; Ober, C. K. *Acta Polym.* **1996**, *48*, 405.
(4) Zhao, Y.; He, J. *Soft Matter* **2009**, *5*, 2686.
(5) Darling, S. B. *Prog. Polym. Sci.* **2007**, *32*, 1152.
(6) Demus, D.; Goodbye, J.; Gray, G. W.; Spiess, H. W.; Vill, V. *Handbook of Liquid Crystals*; Wiley-VCH Verlag: Weinheim, Germany, 1998.
(7) Yu, H. F.; Okano, K.; Shishido, A.; Ikeda, T.; Kamata, K.; Komura, M.; Iyoda, T. *Adv. Mater.* **2005**, *17*, 2184.
(8) Wang, G.; Tong, X.; Zhao, Y. *Macromolecules* **2004**, *37*, 8911.
(9) Yu, H. F.; Shishido, A.; Ikeda, T.; Iyoda, T. *Macromol. Rapid Commun.* **2005**, *26*, 1594.
(10) Zhao, Y.; Qi, B.; Tong, X.; Zhao, Y. *Macromolecules* **2008**, *41*, 3823.
(11) Tian, Y.; Watanabe, K.; Kong, X.; Abe, J.; Iyoda, T. *Macromolecules* **2002**, *35*, 3739.
(12) Morikawa, Y.; Kondo, T.; Nagano, S.; Seki, T. *Chem. Mater.* **2007**, *19*, 1540.
(13) Yu, H. F.; Naka, Y.; Shishido, A.; Ikeda, T. *Macromolecules* **2008**, *41*, 7959.
(14) Yu, H. F.; Asaoka, A.; Shishido, A.; Iyoda, T.; Ikeda, T. *Small* **2007**, *3*, 768.
(15) Yu, H. F.; Li, J.; Ikeda, T.; Iyoda, T. *Adv. Mater.* **2006**, *18*, 2213.
(16) Yu, H. F.; Ikeda, T.; Iyoda, T. *J. Am. Chem. Soc.* **2006**, *128*, 11010.
(17) Yu, H. F.; Shishido, A.; Li, J.; Kamata, K.; Iyoda, T.; Ikeda, T. *J. Mater. Chem.* **2007**, *17*, 3485.
(18) Gray, G.; Herrison, K.; Constant, J.; Hulme, D.; Kirton, J.; Raynes, E. In *Liquid Crystals and Ordered Fluids*; Johnson, J., Porter, R., Eds.; Plenum Press: New York, 1974.
(19) Matyjaszewski, K.; Xia, J. *Chem. Rev.* **2001**, *101*, 2921.
(20) Fasolka, M.; Mayes, A. *Annu. Rev. Mater. Res.* **2001**, *31*, 323.
(21) Bates, F.; Fredrickson, G. *Phys. Today* **1999**, *52*, 32.
(22) Tong, X.; Cui, L.; Zhao, Y. *Macromolecules* **2004**, *37*, 3101.
(23) Ikeda, T. *J. Mater. Chem.* **2003**, *13*, 2037.
(24) Morkved, T.; Lu, M.; Urbas, A.; Ehrichs, E.; Jaeger, H.; Mansky, P.; Russell, T. *Science* **1996**, *273*, 931.
(25) Osuji, C.; Ferreira, P.; Mao, G.; Ober, C.; Vander Sande, J.; Thomas, E. *Macromolecules* **2004**, *37*, 9903.
(26) Bodycomb, J.; Funaki, Y.; Kimishima, K.; Hashimoto, T. *Macromolecules* **1999**, *32*, 2075.
(27) Rosa, C.; Park, C.; Thomas, E.; Lotz, B. *Nature* **2000**, *405*, 433.
(28) Shin, K.; Xiang, H.; Moon, S.; Kim, T.; McCarthy, T.; Russell, T. *Science* **2004**, *306*, 76.
(29) Angelescu, D.; Waller, J.; Register, R.; Chikin, P. *Adv. Mater.* **2005**, *17*, 1878.
(30) Kim, S.; Misner, M.; Xu, T.; Kimura, M.; Russell, T. *Adv. Mater.* **2004**, *16*, 226.
(31) Honeker, C.; Thomas, E.; Albalak, R.; Hajduk, D.; Gruner, S.; Capel, M. *Macromolecules* **2000**, *33*, 9395.
(32) Hasegawa, M. In *Alignment Technologies and Applications of Liquid Crystal Devices*; Takatoh, K., Hasegawa, M., NobuyukiItoh, M., Hasegawa, R., Sakamoto, M., Eds.; Taylor & Francis: London, 2005.
(33) Kim, S.; Solak, H.; Stoykovich, M.; Ferrier, N.; Pablo, J.; Nealey, P. *Nature* **2003**, *424*, 411.

AM900509V